



Droplet digital PCR improves urinary exosomal miRNA detection compared to real-time PCR

Cong Wang^{a,b}, Qiang Ding^b, Pamela Plant^b, Mayada Basheer^c, Chuance Yang^b, Eriny Tawedrous^b, Adriana Krizova^{b,c}, Carl Boulos^b, Mina Farag^b, Yufeng Cheng^{a,*}, George M. Yousef^{b,c,**}

^a Department of Radiation Oncology, Qilu Hospital of Shandong University, Shandong, China

^b Keenan Biomedical Research Centre, Li Ka Shing Knowledge Institute, St Michael's Hospital, Toronto, ON, Canada

^c Department of Laboratory Medicine and Pathobiology, University of Toronto, Toronto, ON, Canada

ARTICLE INFO

Keywords:

ddPCR
qPCR
Optimization
Exosome
Urine
miRNA
Abbreviations
ddPCR
Droplet digital polymerase chain reaction
qPCR
quantitative real time polymerase chain reaction

ABSTRACT

Object: Quantification of urinary miRNAs can be challenging especially for low abundance miRNAs. We aimed to optimize the quantification of urinary exosomal miRNAs and compare the performance efficiency between droplet digital PCR (ddPCR) and real-time quantitative PCR (qPCR).

Methods: We optimized a number of parameters for ddPCR such as annealing temperatures, annealing time and PCR cycle number. We also compared the performance of ddPCR and qPCR.

Results: By comparing the fluorescence amplification separation, the optimal annealing temperature was 59 °C, optimal annealing time was 60s and optimal cycle number was 45 for measuring urinary exosomal miRNAs. ddPCR had much higher technical sensitivity compared to qPCR. The minimal detectable concentration of miR-29a was < 50 copies/μL by ddPCR compared to 6473 copies/μL for qPCR. Also, ddPCR generated more consistent results for serially diluted samples compared to qPCR. ddPCR generated smaller within-run variations than qPCR though this did not reach statistical significance. It also resulted in better reproducibility with smaller between-run variations.

Conclusions: Optimization of urinary exosomal miRNA ddPCR assay is dependent on assessing key variables including experimental annealing temperature and time as well as the number of PCR cycles. ddPCR has a higher sensitivity, reproducibility, and accuracy in comparison to qPCR.

1. Background

Droplet Digital PCR (ddPCR) uses emulsion chemistry to partition 20 μL nucleic acid samples into approximately 20,000 oil-encapsulated nano-droplets. It measures absolute quantities by counting nucleic acid molecules encapsulated in discrete nano-droplets [1]. The ddPCR technology enables higher throughput with lower sample quantity, reagent volumes and overall cost compared with other methods while maintaining sensitivity and precision. ddPCR measures data of reactions end point, employing a positive or negative result for each droplet, thus enabling detection at low concentrations. ddPCR has many other benefits for nucleic acid quantification, such as unparalleled precision, increased signal-to-noise, superior partitioning, removal of PCR efficiency bias, reduced consumable and equipment costs [2,3]. Emerging applications of ddPCR include absolute quantification, single

cell analysis, gene expression and next-generation sequencing [3–8].

Exosomes are 40–100 nm membranous vesicles, which are secreted extracellularly in various body fluids such as plasma, urine, saliva, amniotic fluid and malignant ascites fluids, among others. Exosomes consist of a lipid bilayer surrounding a small cytosol and are loaded with various essential cytosolic proteins, membrane receptors, tetraspanins, immunoglobulins, and nucleic acids [9,10]. Nucleic acids that have been identified in exosomal lumen include mRNAs, microRNAs (miRNAs), and other non-coding RNAs (ncRNAs).

Through extracellular trafficking, exosomal RNAs can communicate with neighboring cells modulating surrounding cellular microenvironment, differentiation and survival [11]. Aberrant miRNA expression has been implicated in disease onset and progression. Consequently, exosomal miRNAs have emerged as potential diagnostic biomarkers [12–15]. For example, a set of exosomal miRNAs can be utilized as

* Correspondence to: Y. Cheng, Department of Radiation Oncology, Qilu Hospital of Shandong University, Jinan, Shandong 250012, China.

** Correspondence to: G. M Yousef, Department of Paediatric Laboratory Medicine, The Hospital for Sick Children, 555 University Avenue, Toronto, ON, M5G 1X8, Canada.

E-mail addresses: qlcyf@sdu.edu.cn (Y. Cheng), george.yousef@sickkids.ca (G.M. Yousef).

<https://doi.org/10.1016/j.clinbiochem.2019.03.008>

Received 20 August 2018; Received in revised form 14 February 2019; Accepted 21 March 2019

Available online 21 March 2019

0009-9120/ © 2019 The Canadian Society of Clinical Chemists. Published by Elsevier Inc. All rights reserved.

diagnostic biomarkers of colorectal cancer [16]. miRNAs can be especially important in urologic tumors as kidney and prostate cancers [17,18]. A number of miRNAs have been shown to have prognostic utility in prostate cancer [19,20]. Exosomal miR-1290 and miR-375 can be utilized as prognostic markers in castration-resistant prostate cancer [21].

Various molecular techniques, for example, quantitative real-time PCR (qPCR), have been used for quantifying miRNA expression. Due to the low abundance of urinary exosomal miRNAs and the lack of reference genes, qPCR is not an optimal method for quantifying the expression of urinary exosomal miRNAs. Drawbacks of qPCR also include that it relies on amplification from a single curve and that Cq value depends on overall reaction efficiency and compatible primer dimer. Interpretation of qPCR data depends on optimal normalization or appropriate reference gene selection.

In the current study, we describe assay optimization for measuring urinary miRNAs by ddPCR and its performance comparison to qPCR. This includes examining key parameters such as buffer conditions, annealing temperature and time, PCR cycles, RT pool models and PCR probe concentrations. We compared the sensitivity, accuracy and reproducibility of ddPCR and qPCR.

2. Materials and methods

2.1. Urine exosomal miRNA isolation and concentration

Pooled urine samples were collected from healthy volunteers. 2 mL of mid-stream morning urine was collected and pooled. Total exosomal miRNAs were isolated and concentrated using Urine Exosomal RNA Isolation Kit and RNA Clean-up and Concentration Micro Kit (Norgen biotek, Thorold, Canada). Cellular, bacterial and residual debris were removed by centrifugation at 2500 rpm for 2 min at room temperature. The supernatant was transferred into a 1.5 mL Eppendorf tube. 300 μ L of “Slurry B1” was added and the mixture was centrifuged to pellet the resin. The pellet resin was re-suspended in 300 μ L of “Lysis Buffer A” and incubated for 15 min at room temperature. The resin was washed with 300 μ L 67% isopropanol and centrifuged according to manufacturer's protocol. The resin in the column was then washed three times with “Wash Solution A”. Bound miRNAs were further eluted with 100 μ L of “Elution Solution A” and centrifuged at 2000 rpm for 2 min followed by 14,000 rpm for 2 min. The columns were then washed and concentrated with 250 μ L of Buffer RL and 200 μ L of 96–100% ethanol. Columns were activated by loading 500 μ L of Column Activation Solution, and the RNA mixture was applied onto the activated column, followed by centrifugation at 14,000 rpm for 1 min. The columns were then washed three times. miRNAs were further eluted with a 15 μ L of “Elution Solution A” and centrifuged at 2000 rpm for 2 min, followed by 14,000 rpm at 1 min. Specimens were stored at -80°C .

2.2. Reverse transcription

Reverse Transcription (RT) was conducted according to manufacturer's instructions (TaqMan MicroRNA Assay kit, Life Technologies California, USA). Briefly, multiplex miRNA RT primers were pooled according to manufacturer's protocol. We compared pools of 1, 2, 4, 8, 16, 32 and 48 pairs of primers. The RT master mix (15 μ L) was prepared by mixing RT primer pool (6.0 μ L), dNTPs with dTTP (0.3 μ L), MultiScribe Reverse Transcriptase (3.0 μ L), 10 \times RT Buffer (1.5 μ L), RNase Inhibitor (0.2 μ L) and Nuclease-free water (1 μ L). 3 μ L of total RNA were added into each tube containing RT reaction mixture for a total reaction volume of 15 μ L. RT was performed for 30 min at 16°C , followed by 30 min at 42°C and 5 min at 85°C . The cDNA library was stored at -80°C .

2.3. Droplet digital PCR

All ddPCR and reaction volumes were performed according to manufacturer's protocol (Bio-Rad, California, USA). PCR reaction mixture (22 μ L) contains Super Mix (11.0 μ L), cDNA (2.0 μ L), Nuclease-free water and Assay Mix. For each miRNA, TaqMan microRNA assay utilized specific primers and probes specific for the mature form of this miRNA. Assay performance was evaluated by using different assay volumes (0.3 μ L, 0.5 μ L, 1.0 μ L, 1.5 μ L to 2.0 μ L).

Reaction plates were loaded into a QX200 Automatic Droplet Generator (Bio-Rad). Each reaction was partitioned into $\sim 20,000$ nanoliter-sized droplets. Droplets were transferred to a 96-well PCR plate for PCR in C1000 Touch thermal cycler with a 96-deep well reaction module. The referenced temperature profile for PCR was 95°C for 60 s, and 45 cycles of 95°C (15 s) then 60°C (60 s). We set pre-degeneration at 95°C for 60 s. Annealing temperature gradients included 65.0°C , 64.4°C , 63.1°C , 61.2°C , 59.0°C , 57.1°C , 55.8°C and 55.0°C . Annealing lasted for 60s or 90s, and cycle numbers included 40 and 45 cycles. Following PCR amplification, the plate containing the droplets was loaded in a QX200 droplet reader, which analyzes each droplet individually using a two-color detection system.

2.4. qPCR

qPCR was performed according to manufacturer's protocol. (Life Technologies California, USA). Pre-amplification reaction mix contains RT Product (2.5 μ L), TaqMan PreAmp Master Mix (2 \times) (12.5 μ L), PreAmp Primer Pool (3.75 μ L) and Nuclease-free water 6.25 μ L. Thermal-cycling conditions are set at 95°C (10 min), 55°C (2 min), 72°C (2 min) and 12 cycles of 95°C (15 s) and 60°C (4 min), followed by 99.9°C (10 min). 175 μ L of 0.1 \times TE, pH 8.0 were added into each mixture to make PreAmp product (Final Volume = 200 μ L). PCR reaction mix includes 1.0 μ L of 20 \times TaqMan[®] MicroRNA Assays, 0.2 μ L of Diluted PreAmp Product, 10.0 μ L of TaqMan[®] Universal Master Mix II and 8.8 μ L of Nuclease-free water. The thermal cycling parameters were 95°C (10 min) followed by 40 cycles of 95°C (15 s) and 60°C (60 s).

2.5. Performance comparison between ddPCR and qPCR

In order to compare the efficiency of ddPCR and qPCR, triplicate experiments were performed using same RNA, testing three miRNAs (miR-29a, miR-30c and miR-652) for three successive days. Each day, RNA was reversed transcribed and the same cDNA was used for ddPCR and qPCR. One sample was serially diluted (1, 1:2, 1:4, 1:8, 1:16, 1:32 and 1:64) to examine the accuracy of ddPCR and qPCR using linear regression (Supplement Fig. 1A). Performances in three successive days were used to compare reproducibility between ddPCR and qPCR (Supplement Fig. 1B). ddPCR provide absolute copy numbers of each miRNA, whereas quantification of copy numbers by qPCR was calculated using standard curves of serial dilutions of oligonucleotide of the specific sequence of each miRNA.

2.6. Statistical analysis

The ddPCR data was analyzed using Qantasoft software (Bio-Rad) version 1.7.4.0917. Optimization was evaluated by the separation between positives and negatives. qPCR results were calculated according to the standard curves. Mean values and standard deviations of ddPCR and qPCR were assessed using student *t*-test. Coefficient of variation (CV) was calculated by dividing standard deviation by mean value. Original samples were diluted successively, and the dilution serials were analyzed. Statistical significance was achieved with *p*-value below 0.05.

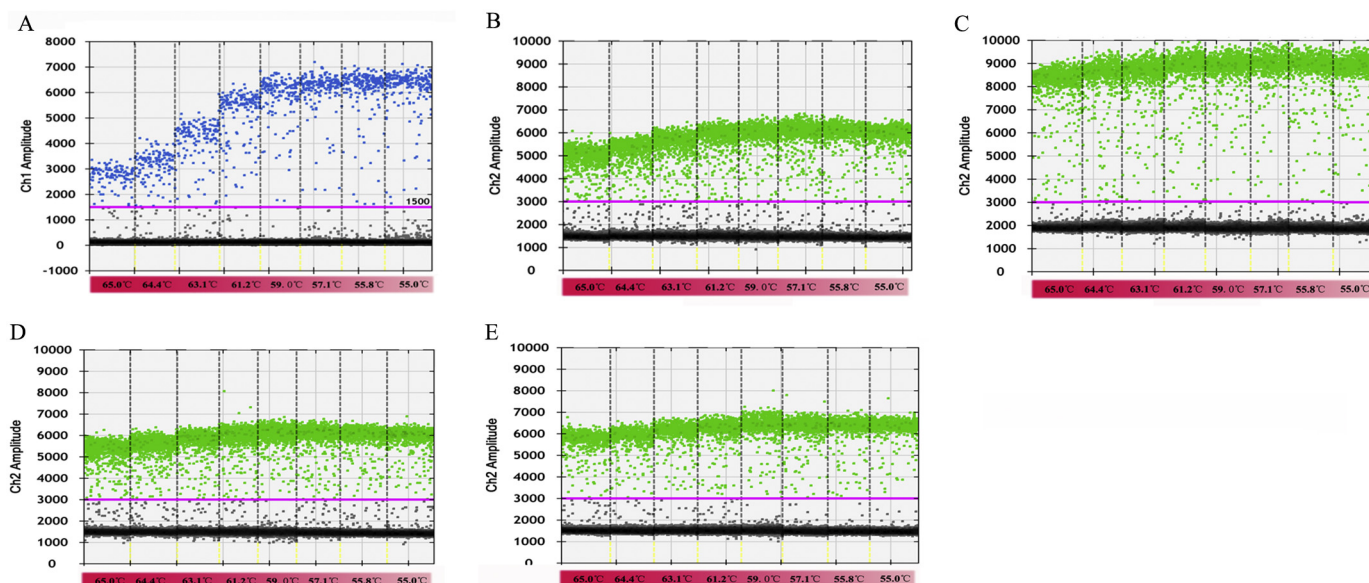


Fig. 1. Annealing temperature, annealing time and PCR cycles affect the amplitude of ddPCR and separation between negative and positive signals. **A.** Blue and green dots represent the positive droplets (above the pink horizontal threshold) for ddPCR with FAM and VIC assays, respectively. Grey dots represent the negative droplets. The X axis represents the number of droplets. Y axis represents signal amplitude. **B-E.** 60 seconds annealing temperature for 45 cycles generated the highest positive signal amplitude and largest separation between positive and negative droplets. Signal amplitude is shown in the y-axis. Green dots represent the VIC fluorescence and grey dots are the negative droplets. **B:** 60 seconds/40 cycles; **C:** 60 seconds/45 cycles; **D:** 90 seconds/40; **E:** 90 seconds/45 cycles.

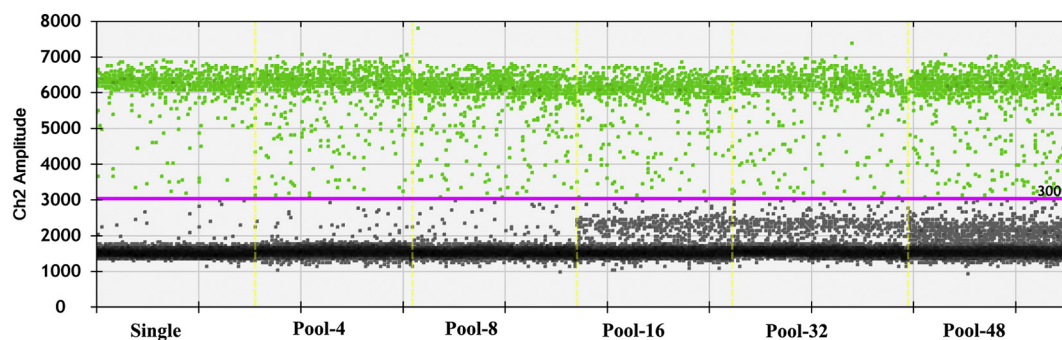


Fig. 2. The effect of pooled RT primers on ddPCR products. We pooled up to 48 primers in one reaction. Pooling of up to 8 primers resulted in insignificant non-specific signal.

3. Results

3.1. Optimization of ddPCR

3.1.1. Annealing temperature

ddPCR partitions nucleic acid samples into thousands of nanoliter-sized droplets (~ 20,000 droplets), and PCR amplification is carried out within each droplet. Annealing temperature has great impact on the separation between positive and negative droplets. Annealing temperature optimization was performed by testing a temperature gradient from 55 °C to 65 °C. As shown in Fig. 1A, different temperatures produced variable signal separation with significant drop in signal separation above 60 °C. Lowering the annealing/extension temperature led to better signal separation, but at the expense of reduced specificity. On the other hand, higher annealing temperatures coincided with loss of positive PCR signaling, and reduced signal separation between positive and negative droplets. We identified 59 °C as the optimal annealing temperature for ddPCR, with greatest signal separation, and the least permissive, non-specific binding.

3.1.2. Annealing time and number of PCR cycles

Annealing time is another variable that affects the performance of the ddPCR assay. We followed the manufacturer's recommended

protocol of using a 2 °C/s ramp rate to ensure each droplet was at the right temperature at each specific step when cycling. We tested four sets of annealing times and cycle numbers, as follows: 60 s/40 cycles (Fig. 1B), 60 s/45 cycles (Fig. 1C), 90 s/40 cycles (Fig. 1D), and 90 s/45 cycles (Fig. 1E). We identified 60 s/45 cycles to generate the largest fluorescence amplitude difference between positive and negative droplets (separations of ~7000 for 60 s/45 cycles group and ~4500 for three other groups).

3.1.3. Reverse transcription primers pooling

An advantage of multiplex platforms is their ability to analyze multiple targets simultaneously with limited amount of sample. This is particularly important when dealing with specimens that are precious and of small amounts, and with the need to assess a multiple biomarkers panel. However, pooled RT primers would impact reverse transcription efficiency and specificity. Consequently, it was critical to determine the optimal pool model with the highest specificity. Initially, we combined up to 48 candidate miRNA RT primers in one reaction. As shown in Fig. 2, multiplexing resulted in increased background signal from non-specific binding. Pooling up to 8 assays, however, resulted in minimum non-specific binding. The non-specific signal significantly increased when pooling 16 or more assays.

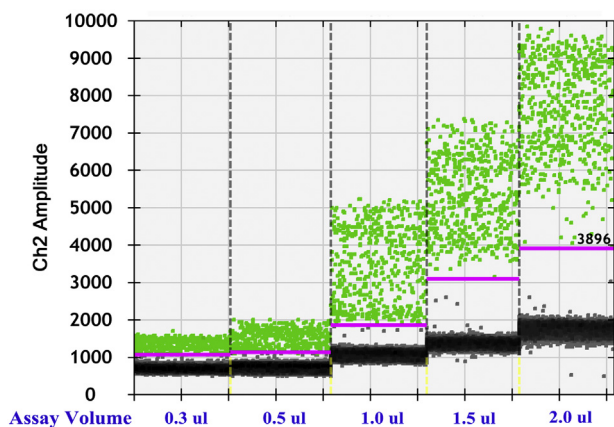


Fig. 3. PCR assay concentration affects the separation between positives and negatives of ddPCR. The separation between positives and negatives increased with the assay volume added in the PCR reaction system. A minimum of 1.0 μL assay is recommended for the continuous run.

3.1.4. miRNA-specific assay concentration

Another key optimization parameter is the assay (probe) concentration. We examined the performance of five PCR assay volumes; 0.3 μL , 0.5 μL , 1.0 μL , 1.5 μL and 2.0 μL . We found that as we raised assay volume, the separation between positive and negative droplets improved, with minimum sufficient separation obtained at 1.0 μL (Fig. 3).

3.2. Comparison between ddPCR and qPCR

To compare accuracy between the qPCR and ddPCR platforms for measuring urinary miRNAs, we compared the expression of three miRNAs of different abundance within the same urine sample by both platforms, using the same experimental design (except for an additional pre-amplification step for qPCR to enhance its sensitivity). Both technologies utilize Taq polymerase in replicating target cDNA with miRNA-specific primer/probe assays. A flow chart of our comparison is shown in Supplementary Fig. 1.

To evaluate assay sensitivity, we compared the expression of three miRNAs with different concentrations; miR-29a (< 100 copies/ μL urine), miR-30c (~1000 copies/ μL urine) and miR-652 (~10,000 copies/ μL urine). As shown in Fig. 4A, ddPCR and qPCR were able to detect miR-30c and miR-652, whereas miR-29a was only detectable by ddPCR. Meanwhile, ddPCR was able to detect miR-29a at an absolute copy number as low as 5–50 copies/ μL . The calculated minimum concentration detectable of miR-29a, miR-30c and miR-652 by qPCR is

6473, 2.42×10^5 and 1.84×10^5 copies/ μL , respectively.

miR-652 was then serially diluted up to 64-fold and expression was examined by both qPCR and ddPCR. As shown in Fig. 4B, the evaluation of copy number by ddPCR displayed a linear miR-652 expression for up to 64-fold dilution, which is 156 copies. qPCR data were not as consistent among various diluted samples. The linear regression equations for ddPCR and qPCR were $y = 1.0018x + 0.1548$ and $y = 0.9067x + 0.9116$, respectively. R^2 values were 0.9969 and 0.9882, respectively. The expected equation is $y = x$. ddPCR generated better consistency with the expected equation compared to qPCR (the coefficient of ddPCR approximates to 1 and its slope (b) approximates to 0). Besides, at 1/64 dilution, qPCR was below detection limit.

Samples were run in triplicates for all measurements to test within-run accuracy and reproducibility. As shown in Fig. 5A, our results show lower within-run CV value (calculated using mean values and standard variations of triple results) in ddPCR versus qPCR, especially in lower target concentrations, however, these differences did not reach statistical significance ($p = .88$ for miR-30c and $p = .18$ for miR-652). We also compared the between-run variation among three consecutive days. CV value (calculated using mean values and standard variations among three continuous days) was used for the variation comparison. We found that CV values of ddPCR were smaller than qPCR for both miRNAs (0.08 vs 0.83 for miR-30c, 0.05 vs 0.78 for miR-652). We also found that miRNA measurements by qPCR were artificially inflated when compared to ddPCR for both miR-30c (Fig. 5B) and miR-652 (Fig. 5C), which also has been previously reported in other publications [22–24]. This could possibly be due to the pre-amplification step needed to boost sensitivity of detection.

4. Discussion

ddPCR has emerged as a new platform for quantifying the expression of exosomal miRNAs. It has been shown to be more accurate and sensitive at detecting targets of lower concentrations compared to qPCR. In addition, ddPCR data is assessed at reaction end points, which offers the advantage of quantification independently from reaction efficiency, standard curves and Cq values.

Despite these benefits, experimental optimization remains essential for ddPCR. ddPCR requires sophisticated assay optimization through analyzing droplet amplitude and scatter along with absolute quantification of nucleic acids. In comparison, in qPCR, data is extracted from a single amplification curve and a Cq value that relies on platform efficiency, selection of appropriate primers probe concentrations and eliminating contaminants. qPCR relies on quantification of the target in a calibrator sample, and assumes no loss of calibrator molecules during the procedure, which is not always the case. Potential inaccuracies of

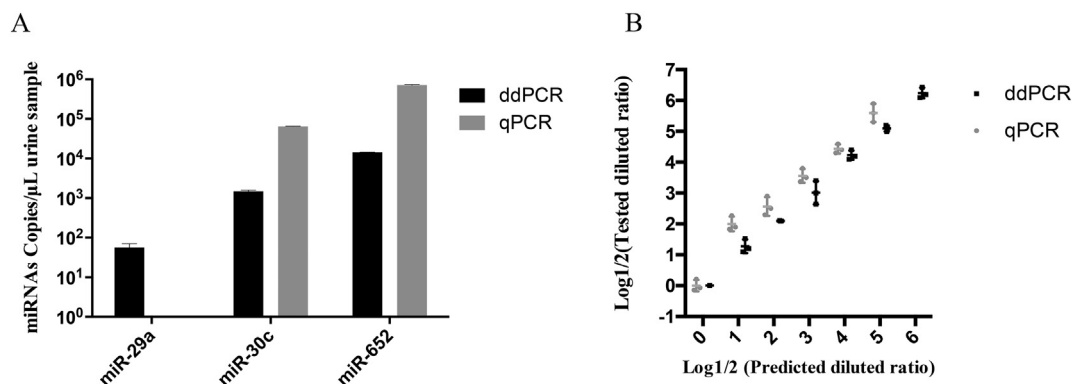


Fig. 4. Comparison between the performance of ddPCR and qPCR. (A) We compared the ability of both methods to measure three miRNAs with three different concentrations; miR-29a (< 100 copies/ μL), miR-30c (~1000copies/ μL) and miR-652 (~10000 copies/ μL urine). The same cDNA was used for both methods. miR-30c and miR-652 were detectable by both technologies, whereas miR-29a was only detectable by ddPCR. (B) Serially diluted samples of miR-652 were used to detect the accuracy of ddPCR and qPCR. ddPCR generated more consistent results compared to qPCR.

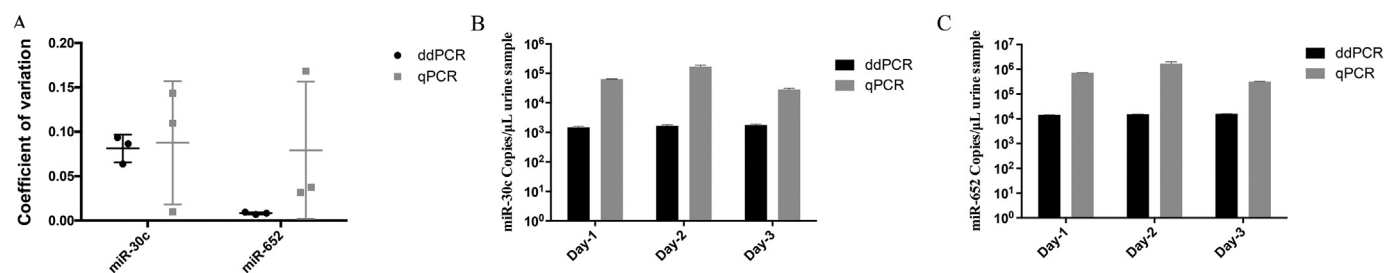


Fig. 5. Comparison of between-run variations of ddPCR and qPCR. (A). ddPCR showed significantly less variations between runs using coefficient of variation (CV) index; (B-C) Expression level of miR-30c and miR-652 in three successive days were shown for both methods. Mean with SD (standard deviation) were shown.

qPCR can occur during initial quantification of the standard, re-suspension and preparation of serial dilutions, reverse transcription and amplification itself [23]. A normalizer or standard curve is required for relative quantification which also could result in the variations of results. Moreover, a pre-amplification step, which is recommended for limited miRNA targets, although could improve sensitivity, can have negative effect on reproducibility [25].

For urinary exosomal miRNAs detection, there is no current consensus for normalization. The formula $\lg 2^{(50-Ct)}$ [26], U6 snRNA [27] or creatinine [28], spike-in miRNA have been used to calculate the relative expression level of urinary miRNAs for qPCR detection [25]. Standard curves outperform reference genes for fluid biomarkers detection using qPCR. Absolute quantification relies strongly on the accuracy of the quantitative standard curves. However, external standards cannot identify or account for inhibitors that could be present within the samples [29].

Parameters considered in ddPCR assay optimization include annealing temperature and time, PCR cycle number, RT assay pooling model and PCR assay concentrations. Our results showed that 59 °C is the optimal annealing temperature for ddPCR with the greatest signal separation. Optimal annealing time of 60 s at 45 cycles generated the largest fluorescence amplitude difference between positive and negative droplets. Pooling of < 16 primers demonstrated optimal partitioning with minimum non-specific binding. Pooling offers a great advantage of being able to measure a number of targets simultaneously from a limited urine sample.

Lower assay volumes can lead to a significant cost reduction. Dilution serials of miRNA-specific PCR assay concentrations identified that with increasing assay volumes, the separation between positive and negative droplets improved, with minimum sufficient separation at 1.0 μL.

We optimized and directly compared the performance between qPCR and ddPCR platforms in nucleic acid quantification. We evaluated sensitivity, precision, linearity and reproducibility of both methods. We found that ddPCR is more sensitive, accurate and of better reproducibility than qPCR. It has been reported that the linearity of ddPCR detection was optimal at target concentrations < 10⁵ copies/μL [30]. miR-29a of low concentration was only detectable by ddPCR but not by qPCR. In this aspect, we recommend ddPCR for the detection of targets with low concentrations. Serially diluted samples were used for the comparison of accuracy between ddPCR and qPCR. ddPCR data was more consistent with the expected results. ddPCR was able to quantify urinary exosomal miRNAs with higher precision and accuracy as compared to qPCR across the entire dilution serials.

Additionally, ddPCR generated lower within-run CVs compared to qPCR though this was not statistically significant. Besides, ddPCR was of better reproducibility with smaller between-run CV values among three continuous days compared with qPCR. This is consistent with a previous report that ddPCR consistently displayed lower variation than qPCR for all miRNAs tested across PCR replicates, RT replicates or serial dilution preparation replicates [22]. Meanwhile, we observed that ddPCR yielded respectively lower values than qPCR. This phenomenon

also has been reported in previous publications [22–24]. These discrepancies may be due to a combination of factors, mentioned above, that can affect the qPCR calibration curve.

However, there are limitations and pitfalls that remain to be eliminated to ensure optimal quantification. Future improvements in experimental outcomes require a bigger cohort with larger sample size and expanded panel of target genes to produce accurate, reproducible data.

In conclusion, this study offers an insight into the key parameters that influence ddPCR performance and its potential application in urinary exosomal miRNAs quantification, as it is rapidly replacing qPCR with superior sensitivity, accuracy, and precision.

Supplementary data to this article can be found online at <https://doi.org/10.1016/j.clinbiochem.2019.03.008>.

Funding

Canadian Urological Oncology Group.
Ontario Molecular Pathology Research network CPTRG-004; CPTRG-015.
Kidney Foundation of Canada KFOC180018.

Acknowledgements

None.

References

- [1] L. Gerdes, A. Iwobi, U. Busch, S. Pecoraro, Optimization of digital droplet polymerase chain reaction for quantification of genetically modified organisms, *Biomol. Detect. Quantif.* 7 (2016) 9–20.
- [2] B.J. Hindson, K.D. Ness, D.A. Masquelier, P. Belgrader, N.J. Heredia, A.J. Makarewicz, L.J. Bright, M.Y. Lucero, A.L. Hiddessen, T.C. Legler, T.K. Kitano, M.R. Hodel, J.F. Petersen, P.W. Wyatt, E.R. Steenblock, P.H. Shah, L.J. Bousse, C.B. Troup, J.C. Mellen, D.K. Wittmann, N.G. Erndt, T.H. Cauley, R.T. Koehler, A.P. So, S. Dube, K.A. Rose, L. Montesclaros, S. Wang, D.P. Stumbo, S.P. Hodges, S. Romine, F.P. Milanovich, H.E. White, J.F. Regan, G.A. Karlin-Neumann, C.M. Hindson, S. Saxonov, B.W. Colston, High-throughput droplet digital PCR system for absolute quantitation of DNA copy number, *Anal. Chem.* 83 (2011) 8604–8610.
- [3] T.C. Dingle, R.H. Sedlak, L. Cook, K.R. Jerome, Tolerance of droplet-digital PCR vs real-time quantitative PCR to inhibitory substances, *Clin. Chem.* 59 (2013) 1670–1672.
- [4] W.W. Chen, L. Balaj, L.M. Liao, M.L. Samuels, S.K. Kotsopoulos, C.A. Maguire, L. Loguidice, H. Soto, M. Garrett, L.D. Zhu, S. Sivaraman, C. Chen, E.T. Wong, B.S. Carter, F.H. Hochberg, X.O. Breakefield, J. Skog, BEAMing and droplet digital PCR analysis of mutant IDH1 mRNA in glioma patient serum and cerebrospinal fluid extracellular vesicles, *Mol. Ther. Nucleic Acids* 2 (2013) e109.
- [5] L. Aigrain, Y. Gu, M.A. Quail, Quantitation of next generation sequencing library preparation protocol efficiencies using droplet digital PCR assays - a systematic comparison of DNA library preparation kits for Illumina sequencing, *BMC Genomics* 17 (2016) 458.
- [6] Y.Y. Kiseleva, K.G. Puitsyn, S.P. Radko, V.G. Zgodina, A.I. Archakov, Digital droplet PCR - a prospective technological approach to quantitative profiling of microRNA, *Biomed. Khim.* 62 (2016) 403–410.
- [7] S.K. Goh, V. Muralidharan, C. Christophi, H. Do, A. Dobrovic, Probe-free digital PCR quantitative methodology to measure donor-specific cell-free DNA after solid-organ transplantation, *Clin. Chem.* 63 (2017) 742–750.
- [8] W.H. Zoutman, R.J. Nell, M. Versluis, D. van Steenderen, R.N. Lalai, J.J. Out-Luiting, M.J. de Lange, M.H. Vermeer, A.W. Langerak, P.A. van der Velden,

- Accurate quantification of T cells by measuring loss of germline T-cell receptor loci with generic single duplex droplet digital PCR assays, *J. Mol. Diagn.* 19 (2017) 236–243.
- [9] L. Zhao, W. Liu, J. Xiao, B. Cao, The role of exosomes and "exosomal shuttle microRNA" in tumorigenesis and drug resistance, *Cancer Lett.* 356 (2015) 339–346.
- [10] L.T. Brinton, H.S. Sloane, M. Kester, K.A. Kelly, Formation and role of exosomes in cancer, *Cell. Mol. Life Sci.* 72 (2015) 659–671.
- [11] H. Butz, R. Nofech-Mozes, Q. Ding, H.W.Z. Khella, P.M. Szabo, M. Jewett, A. Finelli, J. Lee, M. Ordon, R. Stewart, S. Krylov, G.M. Yousef, Exosomal MicroRNAs are diagnostic biomarkers and can mediate cell-cell communication in renal cell carcinoma, *Eur. Urol. Focus* 2 (2016) 210–218.
- [12] X. Huang, T. Yuan, M. Tschannen, Z. Sun, H. Jacob, M. Du, M. Liang, R.L. Dittmar, Y. Liu, M. Liang, M. Kohli, S.N. Thibodeau, L. Boardman, L. Wang, Characterization of human plasma-derived exosomal RNAs by deep sequencing, *BMC Genomics* 14 (2013) 319.
- [13] T. Kogure, I.K. Yan, W.L. Lin, T. Patel, Extracellular vesicle-mediated transfer of a novel long noncoding RNA TUC339: a mechanism of intercellular signaling in human hepatocellular cancer, *Genes Cancer* 4 (2013) 261–272.
- [14] A. Di Meo, J. Bartlett, Y. Cheng, M.D. Pasic, G.M. Yousef, Liquid biopsy: a step forward towards precision medicine in urologic malignancies, *Mol. Cancer* 16 (2017) 80.
- [15] H.W.Z. Khella, N. Daniel, L. Yousef, A. Scorilas, R. Nofech-Mozes, L. Mirham, S.N. Krylov, E. Liandeau, A. Krizova, A. Finelli, Y. Cheng, G.M. Yousef, miR-10b is a prognostic marker in clear cell renal cell carcinoma, *J. Clin. Pathol.* 70 (2017) 854–859.
- [16] X. Zhang, X. Yuan, H. Shi, L. Wu, H. Qian, W. Xu, Exosomes in cancer: small particle, big player, *J. Hematol. Oncol.* 8 (2015) 83.
- [17] M. Tyers, R.J. Haslam, R.A. Rachubinski, C.B. Harley, Molecular analysis of pleckstrin: the major protein kinase C substrate of platelets, *J. Cell. Biochem.* 40 (1989) 133–145.
- [18] A. Fendler, C. Stephan, G.M. Yousef, G. Kristiansen, K. Jung, The translational potential of microRNAs as biofluid markers of urological tumours, *Nat. Rev. Urol.* 13 (2016) 734–752.
- [19] Z. Lichner, A. Fendler, C. Saleh, A.N. Nasser, D. Boles, S. Al-Haddad, P. Kupchak, M. Dharsee, P.S. Nuin, K.R. Evans, K. Jung, C. Stephan, N.E. Fleshner, G.M. Yousef, MicroRNA signature helps distinguish early from late biochemical failure in prostate cancer, *Clin. Chem.* 59 (2013) 1595–1603.
- [20] Z. Lichner, Q. Ding, S. Samaan, C. Saleh, A. Nasser, S. Al-Haddad, J.N. Samuel, N.E. Fleshner, C. Stephan, K. Jung, G.M. Yousef, miRNAs dysregulated in association with Gleason grade regulate extracellular matrix, cytoskeleton and androgen receptor pathways, *J. Pathol.* 237 (2015) 226–237.
- [21] X. Huang, T. Yuan, M. Liang, M. Du, S. Xia, R. Dittmar, D. Wang, W. See, B.A. Costello, F. Quevedo, W. Tan, D. Nandy, G.H. Bevan, S. Longenbach, Z. Sun, Y. Lu, T. Wang, S.N. Thibodeau, L. Boardman, M. Kohli, L. Wang, Exosomal miR-1290 and miR-375 as prognostic markers in castration-resistant prostate cancer, *Eur. Urol.* 67 (2015) 33–41.
- [22] C.M. Hindson, J.R. Chevillet, H.A. Briggs, E.N. Gallichotte, I.K. Ruf, B.J. Hindson, R.L. Vessella, M. Tewari, Absolute quantification by droplet digital PCR versus analog real-time PCR, *Nat. Methods* 10 (2013) 1003–1005.
- [23] P. Campomenosi, E. Gini, D.M. Noonan, A. Poli, P. D'Antona, N. Rotolo, L. Dominion, A. Imperatori, A comparison between quantitative PCR and droplet digital PCR technologies for circulating microRNA quantification in human lung cancer, *BMC Biotechnol.* 16 (2016) 60.
- [24] M.A. Sze, M. Abbasi, J.C. Hogg, D.D. Sin, A comparison between droplet digital and quantitative PCR in the analysis of bacterial 16S load in lung tissue samples from control and COPD GOLD 2, *PLoS One* 9 (2014) e110351.
- [25] J. Jarry, D. Schadendorf, C. Greenwood, A. Spatz, L.C. van Kempen, The validity of circulating microRNAs in oncology: five years of challenges and contradictions, *Mol. Oncol.* 8 (2014) 819–829.
- [26] Y. Liu, G. Gao, C. Yang, K. Zhou, B. Shen, H. Liang, X. Jiang, Stability of miR-126 in urine and its potential as a biomarker for renal endothelial injury with diabetic nephropathy, *Int. J. Endocrinol.* 2014 (2014) 393109.
- [27] H.W. Kao, C.Y. Pan, C.H. Lai, C.W. Wu, W.L. Fang, K.H. Huang, W.C. Lin, Urine miR-21-5p as a potential non-invasive biomarker for gastric cancer, *Oncotarget* 8 (2017) 56389–56397.
- [28] Y.Y. Hu, W.D. Dong, Y.F. Xu, X.D. Yao, B. Peng, M. Liu, J.H. Zheng, Elevated levels of miR-155 in blood and urine from patients with nephrolithiasis, *Biomed. Res. Int.* 2014 (2014) 295651.
- [29] S.A. Bustin, R. Mueller, Real-time reverse transcription PCR (qRT-PCR) and its potential use in clinical diagnosis, *Clin. Sci. (Lond.)* 109 (2005) 365–379.
- [30] L.B. Pinheiro, V.A. Coleman, C.M. Hindson, J. Herrmann, B.J. Hindson, S. Bhat, K.R. Emslie, Evaluation of a droplet digital polymerase chain reaction format for DNA copy number quantification, *Anal. Chem.* 84 (2012) 1003–1011.